



doi:10.1016/j.gca.2003.09.024

Kinetic isotopic fractionation during carbonate dissolution in laboratory experiments: implications for detection of microbial CO₂ signatures using δ¹³C-DIC

MARK SKIDMORE,^{1,†,*} MARTIN SHARP,¹ and MARTYN TRANTER²¹Department of Earth and Atmospheric Sciences, University of Alberta, Edmonton, Alberta, Canada, T6G 2E3²Bristol Glaciology Centre, School of Geographical Sciences, University of Bristol, Bristol, BS8 1SS, United Kingdom

(Received December 3, 2002; accepted in revised form September 26, 2003)

Abstract—Laboratory experiments on reagent-grade calcium carbonate and carbonate rich glacial sediments demonstrate previously unreported kinetic fractionation of carbon isotopes during the initial hydrolysis and early stages of carbonate dissolution driven by atmospheric CO₂. There is preferential dissolution of Ca¹²CO₃ during hydrolysis, resulting in δ¹³C-DIC values that are significantly lighter isotopically than the bulk carbonate. The fractionation factor for this kinetic isotopic effect is defined as ε_{carb}. ε_{carb} is greater on average for glacial sediments (−17.4‰) than for calcium carbonate (−7.8‰) for the < 63 μm size fraction, a sediment concentration of 5 g L^{−1} and closed system conditions at 5°C. This difference is most likely due to the preferential dissolution of highly reactive ultra-fine particles with damaged surfaces that are common in subglacial sediments. The kinetic isotopic fractionation has a greater impact on δ¹³C-DIC at higher CaCO₃:water ratios and is significant during at least the first 6 h of carbonate dissolution driven by atmospheric CO₂ at sediment concentrations of 5 g L^{−1}. Atmospheric CO₂ dissolving into solution following carbonate hydrolysis does not exhibit any significant equilibrium isotopic fractionation for at least ~ 6 h after the start of the experiment at 5°C. This is considerably longer than previously reported in the literature. Thus, kinetic fractionation processes will likely dominate the δ¹³C-DIC signal in natural environments where rock:water contact times are short <6–24 h (e.g., glacial systems, headwaters in fluvial catchments) and there is an excess of carbonate in the sediments. It will be difficult apply conventional isotope mass balance techniques in these types of environment to identify microbial CO₂ signatures in DIC from δ¹³C-DIC data. Copyright © 2004 Elsevier Ltd

1. INTRODUCTION

Rates of chemical weathering in glaciated catchments are comparable to those in nonglacial catchments with similar specific runoff (Anderson et al., 1997). The abundant supply of freshly comminuted, silt-sized sediment apparently compensates for the low temperatures and the limited contact times between water and sediment during the summer melt season. The main geochemical weathering reactions in glacial environments appear to be largely independent of bedrock lithology (e.g., Sharp, 1996). Reactive minerals, such as sulfides and carbonates which are often present in trace quantities (<0.1%) in the bedrock, have a dominant role in the rock-water interactions which occur, so determining the chemical composition of the meltwaters (Tranter et al., 1993). This assertion is consistent with experimental studies on freshly ground granites (as found in subglacial environments), which demonstrate that calcite weathering predominates over silicate weathering for the first 1000 h, even when CaCO₃ comprises as little as 0.03% of the bedrock (White et al., 1999).

Earlier studies of chemical weathering in subglacial environments assumed that atmospheric CO₂ has a major role in supplying protons for weathering reactions (Gibbs and Kump, 1994; Sharp et al., 1995; Hodson et al., 2000). However, recent work on δ¹⁸O-SO₄^{2−} in runoff from Haut Glacier d'Arolla,

Switzerland, suggests that parts of the glacier bed become anoxic, and that there is little ingress of atmospheric gases in water-filled subglacial environments (Bottrell and Tranter, 2002). If this is the case, the major source of dissolved inorganic carbon (DIC) in glacial runoff is the bedrock, from carbonates and the microbial respiration of organic carbon. Microbial populations have been found in association with subglacial sediments from two Swiss glaciers (Sharp et al., 1999) and microbial oxidation of organic C at 0.3°C has been demonstrated using subglacial sediments from John Evans Glacier, Ellesmere Island (Skidmore et al., 2000).

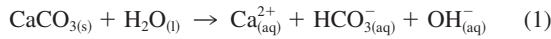
δ¹³C-DIC in runoff has been utilized to determine the relative magnitude of microbial (soil) and atmospheric CO₂ sources in unglaciated catchments (Amiotte-Suchet et al., 1999; Telmer and Veizer, 1999). The main potential sources of DIC in glacial runoff (carbonate minerals, atmospheric CO₂ and CO₂ from the microbial oxidation of organic carbon) usually have significantly different δ¹³C values (Faure, 1986). Hence, δ¹³C-DIC of glacial runoff has the potential to quantify the contribution of CO₂ from the various sources. Confounding factors include the nonstoichiometric or selective dissolution of carbonates (Fairchild and Killawee, 1995), resulting in δ¹³C-DIC values that are not representative of the bulk carbonate. To date, the effects of kinetic processes on δ¹³C-DIC during the early phases of carbonate dissolution have not been reported in the literature.

A series of free drift weathering experiments were conducted to investigate whether kinetic fractionation of carbon isotopes occurs during carbonate hydrolysis and/or carbonate dissolution driven by atmospheric CO₂. These experiments were designed to simulate (sub)glacial chemical weathering under in situ conditions,

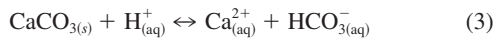
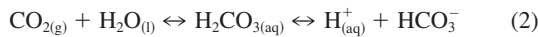
* Author to whom correspondence should be addressed (skidmore@montana.edu).

† Present address: Department of Earth Sciences, 200 Traphagen Hall, Montana State University, Bozeman, MT 59717, USA.

where active subglacial crushing and grinding of bedrock continually renew the supply of trace mineral components of bedrock and generate ultra-fine particles with damaged surfaces that are highly reactive (Blum and Erel, 1995; Anderson et al., 1997, 2000; Brantley et al., 1998). The experiments were therefore performed using silt and clay sized sediment ($<63 \mu\text{m}$). Pure, powdered reagent-grade calcium carbonate (hereafter CaCO_3) and carbonate-rich subglacially derived sediments from John Evans Glacier, Ellesmere Island, Canada were used to compare and contrast the behavior of synthetic and natural carbonate. The experiments were carried out under both closed and open system conditions. Closed system experiments were conducted in water filled sealed bottles that prevented any exchange with the atmosphere. Open system experiments had free access to the atmosphere throughout. Effectively, the closed system conditions provide a measure of the isotopic fractionation associated with carbonate hydrolysis (Eqn. 1), whereas the open system conditions provide information on additional isotopic fractionation effects due to carbonate dissolution driven by the ingress of atmospheric CO_2 (Eqns. 2 and 3). Carbonate hydrolysis



Carbonate dissolution driven by the carbonation reaction

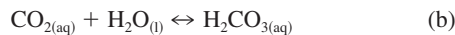


1.1. Isotopic Fractionation and Carbonate Equilibria

The PCO_2 (which reflects the partial pressure of CO_2 in a hypothetical atmosphere with which the waters are in equilibrium) of glacial meltwaters frequently indicates that chemical equilibration of DIC with the atmosphere has not been achieved, and that physical or kinetic barriers have limited CO_2 exchange with the atmosphere (Fairchild et al., 1994). Isotopic exchange of $^{13}\text{CO}_2$ and $^{12}\text{CO}_2$ occurs concurrently with CO_2 exchange. However, isotopic equilibrium is often not achieved as quickly as chemical equilibrium (Szaran, 1997). So, it is reasonable to infer that glacial meltwaters that are not in chemical equilibrium with atmospheric PCO_2 may not be in isotopic equilibrium with the atmosphere. It follows that an understanding of reaction rates in the DIC-carbonate system and the associated kinetic and equilibrium isotopic fractionations is important to interpret the $\delta^{13}\text{C}$ -DIC of glacial meltwaters.

1.1.1. Chemical Equilibria in the Carbonate System

Carbonate equilibria can be described using the following equations (Stumm and Morgan, 1996):



The slowest component of this set of reactions is the gas transfer reaction a, (Dreybrodt et al., 1996). This reaction is frequently slower than other reactions that produce or consume

CO_2 in the aqueous phase, such as calcite dissolution and precipitation (Stumm and Morgan, 1996). Reaction b is reported to equilibrate on the order of 20–200 s (following Mills and Urey, 1940) in stirred solutions. Reactions c and d are reported to equilibrate on the order of seconds (Stumm and Morgan, 1996). The majority of DIC at the pH of glacial waters, typically pH 6–9 (Raiswell, 1984), is as HCO_3^- and thus the isotopic fractionation between $\text{CO}_{2(g)}$ and HCO_3^- ($\epsilon_{\text{HCO}_3\text{-g}}$) is of greatest interest to this study.

1.1.2. Equilibrium Isotope Fractionations in the Carbonate System

Some glacial waters are in chemical equilibrium with the atmosphere as indicated by a PCO_2 of $10^{-3.5}$ atm at sea level and thus, may also be in isotopic equilibrium. There are equilibrium isotopic fractionations for all stages of the dissolution and dissociation of CO_2 in solution, assuming that isotopic equilibrium has been achieved. However, it is the slower reactions that are likely to cause nonequilibrium fractionation effects (Equations a and b, section 1.1.1.). Equilibrium constants relating the $\delta^{13}\text{C}$ fractionations for the reactions $\text{CO}_{2(g)}\text{-CO}_{2(aq)}$, $\text{CO}_{2(g)}\text{-HCO}_3^-(aq)$ and $\text{CO}_{2(g)}\text{-CO}_3^{2-}(aq)$ have been determined experimentally (e.g., Deines et al., 1974) resulting in the fractionation factors ($\epsilon_{\text{g-s}}$), ($\epsilon_{\text{HCO}_3\text{-g}}$) and ($\epsilon_{\text{CO}_3\text{-g}}$) respectively. These fractionation factors are temperature dependent, being greatest at 0°C , which is the approximate temperature for geochemical reactions in subglacial environments. Fractionation occurs during the hydration stage of the reaction $\text{CO}_{2(g)}\text{-HCO}_3^-(aq)$ (Eqn. b) (Zhang et al., 1995) and has been determined experimentally by numerous workers (Deuser and Degens, 1967; Wendt, 1968; Mook et al., 1974; Zhang et al., 1995; Szaran, 1997). $\epsilon_{\text{HCO}_3\text{-g}}$ at isotopic equilibrium has been measured as 10.2‰ at 5°C (Mook et al., 1974; Zhang et al., 1995), which agrees well with the determinations of 9.7‰ and 9.9‰ at 7°C , Wendt (1968) and Szaran (1997) respectively. Deuser and Degens (1967) present a value for $\epsilon_{\text{HCO}_3\text{-g}}$ that is 1.5‰ less than the other studies at 5°C and is therefore ignored. The experiments in this study were carried out at 5°C and an equilibrium $\epsilon_{\text{HCO}_3\text{-g}}$ value of 10.2‰ was used in all calculations.

1.1.3. Kinetic Fractionations in the Carbonate System

Kinetic fractionation processes occur before isotopic equilibrium is achieved in the DIC system. Kinetic fractionation factors for these processes have been determined experimentally. Vogel et al. (1970) and Zhang et al. (1995) demonstrate a kinetic fractionation of CO_2 (ϵ_k), in the initial stages of CO_2 transfer across the gas-water interface. At 5°C , ϵ_k is -1.0% . This is in addition to $\epsilon_{\text{g-s}}$ and presumably is carried through to the HCO_3^- phase during CO_2 hydration. Szaran (1997) reveals another kinetic fractionation effect. $\epsilon_{\text{HCO}_3\text{-g}}$ is significantly reduced from the equilibrium value in the initial stages of the equilibration between $\text{CO}_{2(g)}$ and $\text{HCO}_3^-(aq)$ (e.g., after 1 h it is 2‰ compared to 9.9‰ at equilibrium). $\epsilon_{\text{HCO}_3\text{-g}}$ increases through time, rapidly at first, slowing as it approaches the equilibrium value. Isotopic equilibrium is achieved in ~ 13 h for an unstirred solution at 7°C . Stirring the solution reduces equilibration time to ~ 1.8 h (Szaran, 1997). Temperatures in

subglacial environments would be lower (0°C), so longer equilibration times would be expected due to the lower energy of the molecules in the solution. Hence, it seems reasonable to anticipate that $\epsilon_{\text{HCO}_3\text{-g}}$ will be lower than the equilibrium value in the initial stages of carbonate weathering in the subglacial environment.

2. MATERIALS AND METHODS

Initial experiments using reagent-grade powdered calcium carbonate (CaCO_3) with concentrations in the range (0.01–10 g L^{-1}) demonstrated that the shaken solutions remained in chemical equilibrium with the overlying atmosphere at concentrations $< 0.1 \text{ g L}^{-1}$ (Sharp, unpublished data). At concentrations $> 0.1 \text{ g L}^{-1}$, the solutions initially exhibited low PCO_2 values, returning to equilibrium on a timescale of days. At concentrations $> 0.5 \text{ g L}^{-1}$, the variability in the saturation index for calcite (SI_{cc}) and PCO_2 through time was independent of sediment concentration. Hence, sediment concentrations of 0.01 g L^{-1} and 5 g L^{-1} were chosen to examine the isotopic behavior of carbonate dissolution in systems with both equilibrium and disequilibrium PCO_2 values. These values also cover the range of suspended sediment concentrations observed in the field in Arctic (John Evans Glacier, Ellesmere Island, Canada), and Alpine (Haut Glacier d'Arolla, Switzerland), catchments (Brown et al., 1994; Skidmore, 1995).

Three sets of weathering experiments were undertaken using glacially derived suspended sediment from John Evans Glacier, at concentrations of 5 g L^{-1} (both open and closed system conditions) and 0.01 g L^{-1} (open system conditions only). The sediment was sampled in the proglacial area from overbank fines deposited by active subglacial stream outlets. The dominant minerals are calcite, dolomite and gypsum, determined using X-ray diffraction. Three parallel sets of experiments were performed under the same conditions as for the glacial sediment using reagent-grade powdered CaCO_3 (Fisher Chemicals). Grain size analysis of the $< 300 \mu\text{m}$ fraction of sediment from debris-rich basal ice at John Evans Glacier revealed only grains $< 50 \mu\text{m}$. The analysis was performed using a Sedigraph (Micromeritics 5100) with solutions presaturated with respect to calcite and dolomite to prevent dissolution of finer grain sizes during measurement (Fairchild et al., 1999). Therefore, the $< 63 \mu\text{m}$ fraction of CaCO_3 and glacial sediment was used in the weathering experiments to simulate conditions analogous to those at the glacier bed. All powders (both sediment and CaCO_3) were combusted overnight at 550°C to remove any organic carbon and to sterilize the samples. The polypropylene bottles used in the experiments were triple rinsed with 0.2 μm filtered deionized water and filled brim full (c. 300 mL), capped and placed in the fridge to cool to ambient temperature, $\sim 5^\circ\text{C}$. A small air bubble ($\sim 3 \text{ cm}^3$), remained in the bottle head space in the closed system experiments. 50 mL was decanted from the bottles (leaving 250 mL) to prevent spillage during gyratory shaking for the open system experiments, and the bottles remained uncapped throughout these experiments. Sediment weights were adjusted between open and closed system experiments to account for the difference in water volumes, providing a final concentration of 5 g L^{-1} in both. Ten bottles were prepared for each set of experiments, one for each time step (0.017, 0.033, 0.08, 0.17, 0.33, 1, 2, 6, 24, 168 h). The sediment was added to the bottles, which were placed in the fridge and shaken at 200 rpm in a gyratory shaker. After the requisite time had elapsed, samples were collected and immediately vacuum filtered through 0.45 μm cellulose nitrate filter membranes. The pH of the filtrate was measured immediately after filtration using an Orion 290A pH meter fitted with a Ross Sure-flow pH electrode, calibrated using Orion low ionic strength buffers. Filtered samples were transferred into 20 mL polypropylene vials for cation and anion analysis, and into either autoclaved 45 mL EPA vials or autoclaved 120 mL serum bottles for $\delta^{13}\text{C}$ -DIC analysis. All samples were stored at 4°C before analysis. Major anion (Cl^- , NO_3^- and SO_4^{2-}) and cation (Na^+ , K^+ , Mg^{2+} and Ca^{2+}) concentrations were determined by ion chromatography (Skidmore and Sharp, 1999). Alkalinity was determined by charge balance (alkalinity = sum of cations (Σ^+) – sum of anions (Σ^-)) from the ion chromatography results. DIC speciation, PCO_2 and saturation indices for calcite (SI_{cc}) and dolomite (SI_{dol}) were computed using PHREEQC (Parkhurst and Appelo, 1999).

Water samples for $\delta^{13}\text{C}$ -DIC analysis were withdrawn from the collection vessels using needles and syringes, displacing the water with He gas to minimize any potential CO_2 exchange with the atmosphere. The sample was injected into preevacuated reaction vessels containing 1–5 mL 100% H_3PO_4 , depending on sample size. Injection volumes of water varied from 7 to 125 mL, depending on DIC concentration. The evolved head space gas from the reaction vessel was injected into an HP Series II 5890 gas chromatograph for gas separation and passed through a Mat Combustion Interface. The purified and dehumidified CO_2 was directed to a Finigan Mat 252 mass spectrometer for isotope ratio measurement. The head space gas was injected at least twice for the majority of samples to check sample reproducibility. Internal precision was $\pm 0.5\%$. Fridge air was sampled using serum bottles that were left open in the fridge for 24 h. The bottles were then sealed and the $\delta^{13}\text{C}$ of CO_2 was analyzed using GC-IRMS as above.

The $\delta^{13}\text{C}$ of carbonate in the $< 63 \mu\text{m}$ glacial sediment and CaCO_3 (Fisher Chemicals) was determined as follows. Weighed, powdered samples were reacted under vacuum with 100% H_3PO_4 to liberate CO_2 from carbonate minerals present in the sample (McCrea, 1950). The isotope ratio of the CO_2 was determined on a Finigan Mat 252 Mass Spectrometer. Standard correction procedures were used (Craig, 1957) and the results are reported relative to the V-PDB standard. Duplicate analyses were undertaken for all samples, following the full analytical procedure using separate reaction vessels for each aliquot. The range between duplicates was 0.1%.

3. RESULTS AND DISCUSSION

3.1. Geochemical Properties

The CaCO_3 experiments present the simplest case for observing the isotopic changes during carbonate weathering, since a) only calcium and DIC are present in solution, and b) there is likely limited variability between the sample aliquots for successive time steps due to the relative homogeneity of the synthetic CaCO_3 . By contrast, the sediment experiments use natural, glacially ground material that contains a mixture of calcite, dolomite and gypsum with greater heterogeneity in carbonate content, carbonate mineralogy and grain size distribution. The geochemical evolution of the waters is therefore more complex, and there is potentially more sample variability between time steps. The temporal variations in geochemical properties (alkalinity, PCO_2 , SI_{cc} , SI_{dol} and Ca^{2+} and Mg^{2+} concentrations) during the weathering experiments are shown in Figure 1. Only alkalinity and PCO_2 are plotted for the 0.01 g L^{-1} experiments.

3.1.1. The 5 g L^{-1} Closed System Experiments

The geochemical indices (alkalinity, PCO_2 and SI_{cc}) are reasonably constant over time in the CaCO_3 experiment ($\sim 220 \mu\text{Eq L}^{-1}$, 10^{-6} atm and -0.1 respectively) (Figs. 1a–c). These values are consistent with theoretical predictions from PHREEQC for carbonate hydrolysis, indicating that only carbonate hydrolysis has occurred in these experiments. These geochemical indices (and SI_{dol}) also remain relatively constant after 0.06 h in the sediment experiments. However, the values differ from those of the CaCO_3 experiments (alkalinity $\sim 420 \mu\text{Eq L}^{-1}$, $\text{PCO}_2 \sim 10^{-7}$ atm, SI_{cc} and $\text{SI}_{\text{dol}} \sim +0.6$). The higher alkalinity and the decreased PCO_2 result from a combination of calcite and dolomite hydrolysis in the sediment experiment. 290 $\mu\text{Eq L}^{-1}$ of alkalinity are produced during the first 0.017 h of which $\sim 220 \mu\text{Eq L}^{-1}$ is from calcite hydrolysis, the remainder is from dolomite hydrolysis. Dolomite hydrolysis continues until 0.06 h adding a further $\sim 130 \mu\text{Eq L}^{-1}$ of

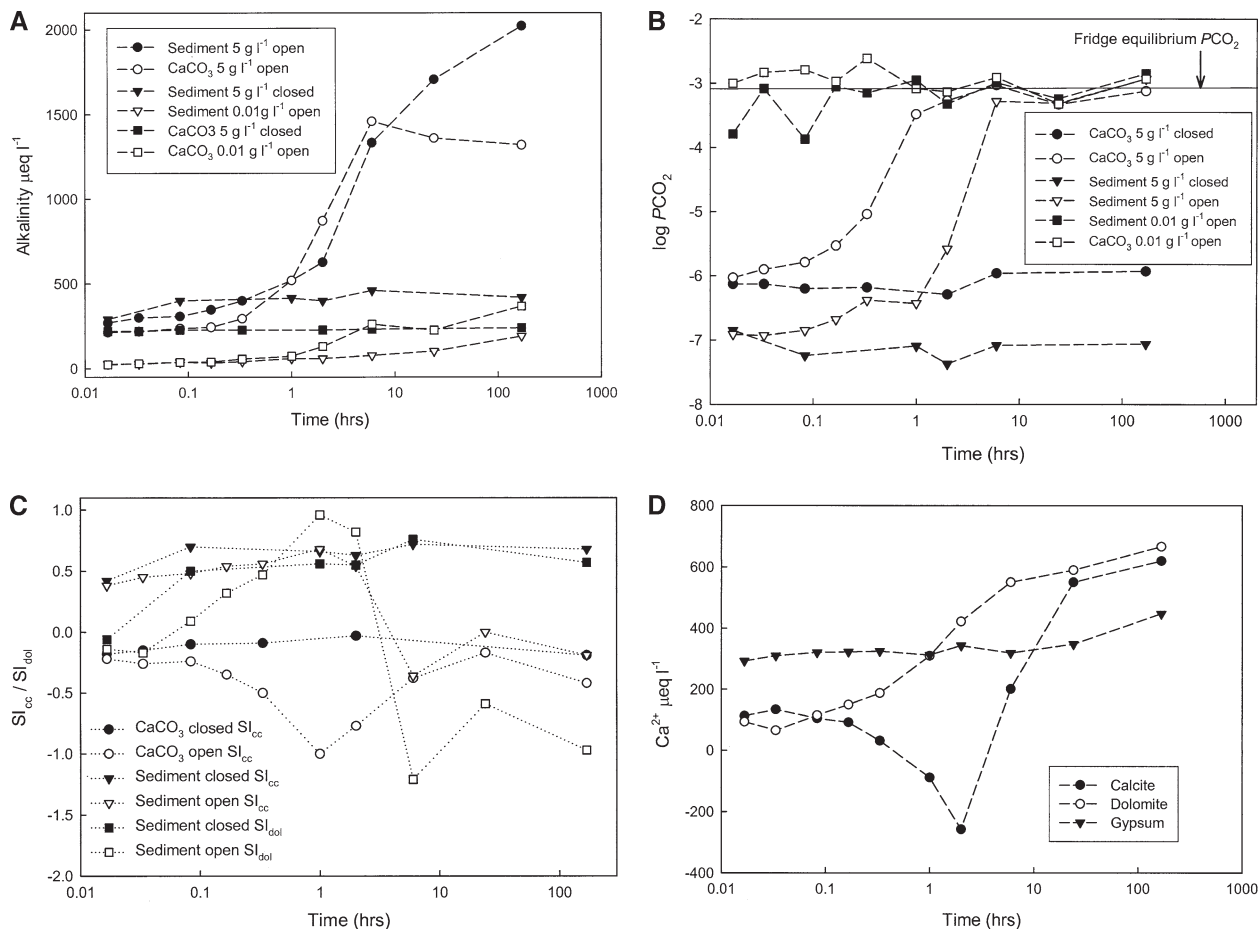


Fig. 1. "Free drift" weathering experiments. (a) Alkalinity vs. time (all experiments), (b) PCO_2 vs. time (all experiments), the fridge equilibrium PCO_2 is based on an average of the 2–168 h values, where a steady state has been attained. (c) SI_{cc} and SI_{dol} vs. time for 5 g L⁻¹ experiments and (d) Ca^{2+} concentrations from calcite, dolomite and gypsum weathering in the open system 5 g L⁻¹ sediment experiment. The proportions of Ca^{2+} from dolomite and calcite are calculated as follows: Calcite Ca^{2+} = Total Ca^{2+} - gypsum Ca^{2+} - dolomite Ca^{2+} . Gypsum Ca^{2+} : all SO_4^{2-} is assumed to arise from gypsum dissolution producing an equivalent amount of Ca^{2+} . Dolomite Ca^{2+} : all Mg^{2+} is assumed to arise from dolomite dissolution producing an equivalent amount of Ca^{2+} . The remainder of the Ca^{2+} arises from calcite dissolution. Negative values likely reflect calcite precipitation.

alkalinity. Thereafter, alkalinity is relatively constant. The lag for dolomite hydrolysis relative to calcite hydrolysis is not unexpected since Chou et al. (1989) demonstrate that dolomite dissolution is approximately an order of magnitude slower than calcite dissolution at pH 9–9.5. Assuming that all sulfate is from gypsum dissolution, this process contributes $\sim 320 \pm 13 \mu\text{Eq L}^{-1}$ of calcium and sulfate in all time steps in the 5 g L⁻¹ sediment experiments. The higher SI_{cc} values and $SI_{dol} > 0$ in the sediment experiment relative to the CaCO₃ experiment are due to a combination of calcite and dolomite hydrolysis and the contribution of calcium from gypsum dissolution.

3.1.2. The 5 g L⁻¹ Open System Experiments

The geochemical indices after 0.017 h in both the CaCO₃ and sediment experiments are close to their closed system counterparts. This indicates that carbonate hydrolysis is the initial weathering process in the open system experiments. Thereafter, changes in the geochemical indices reflect the effects of carbonate dissolution due to carbonate dissolution driven by the

influx of atmospheric CO₂. CO₂ ingress is relatively rapid following carbonate hydrolysis in the CaCO₃ experiments. As a result, alkalinity and PCO_2 increase, and SI_{cc} decreases. The system reaches a near steady state after 6 h that is slightly undersaturated with respect to calcite in the CaCO₃ experiments (Figs. 1a–c).

Chemical weathering processes in the sediment experiment are less straightforward. Calcite hydrolysis and a degree of dolomite hydrolysis occur initially, coupled with gypsum dissolution. The input of calcium and sulfate is relatively constant in time steps 0.017–6 h $\sim 320 \pm 17 \mu\text{Eq L}^{-1}$ (Fig. 1d) and is almost identical in magnitude to that in the closed system experiments. The amount of dolomite hydrolysis and degree of supersaturation with respect to dolomite do not, however, approach those observed in the closed system experiments until 0.33 h have elapsed. Dolomite dissolution continues after this, even though the solution is supersaturated with respect to dolomite until 2 h have elapsed (Figs. 1c,d). Mass balance calculations suggest that calcite precipitation starts 0.17 h after

the start of the experiment and is at a maximum between 1 and 2 h as indicated by the negative Ca^{2+} values (Fig. 1d). SI_{cc} is > 0.5 during this period which supports the notion of calcite precipitation (Fig. 1c). PCO_2 values are still far from equilibrium for significantly longer in the sediment experiment than in the CaCO_3 experiment (Fig. 1b).

3.1.3. The 0.01 g L⁻¹ Open System Experiments

Carbonate hydrolysis produced at least an order of magnitude less alkalinity in the 0.01 g L⁻¹ open system experiments than the 5 g L⁻¹ experiments. Only in the sediment experiment did carbonate hydrolysis result in a reduction of PCO_2 from equilibrium for the first 0.06 h. Overall, the CaCO_3 experiment produced higher alkalinity than the sediment experiment.

3.2. Chemical and Isotope Equilibrium

The closed system 5 g L⁻¹ weathering experiments both produced low PCO_2 values ($< 10^{-6}$ atm) at all time steps (Fig. 1b). The open system 5 g L⁻¹ experiments initially produced low PCO_2 values similar to those in the closed system experiments (Fig. 1b). PCO_2 , however, returned to equilibrium with the fridge atmosphere after 2 h (CaCO_3) and 24 h (sediment). Solutions were at, or near to, chemical equilibrium with the fridge atmosphere throughout the 0.01 g L⁻¹ experiments with both CaCO_3 and sediment (Fig. 1b).

The temporal variations in $\delta^{13}\text{C}$ -DIC for all the weathering experiments are shown in Figures 2a–c. Bulk carbonate $\delta^{13}\text{C}$ values were -3.3‰ for CaCO_3 and an average of -2.15‰ for the sediment ($\delta^{13}\text{C}$ calcite = -1.6‰ and $\delta^{13}\text{C}$ dolomite = -2.7‰). Fridge air had an average $\delta^{13}\text{C}$ - CO_2 value of -13.8‰ . The corresponding equilibrium $\delta^{13}\text{C}$ -DIC value is -3.6‰ at 5°C. A significant negative departure from the equilibrium $\delta^{13}\text{C}$ values was evident at all time steps in the closed system experiments with both CaCO_3 and sediment (Fig. 2a). The solution was close to chemical equilibrium after only 1 h, and equilibrium was attained after 2 h in the open system 5 g L⁻¹ CaCO_3 experiment (Fig. 1b). Isotope equilibrium was attained after > 6 h and < 24 h (Fig. 2b). The solution approached chemical equilibrium after 6 h, but isotope equilibrium was not achieved even after 168 h in the 5 g L⁻¹ sediment experiment (Fig. 2b). Isotope equilibrium was almost achieved after 24 h in both the 0.01 g L⁻¹ CaCO_3 and sediment experiments (Fig. 2c). These results confirm that isotope equilibrium significantly lagged chemical equilibrium in the open system experiments. Moreover, the 0.01 g L⁻¹ experiments demonstrate that significant departures from isotope equilibrium occurred even though there was no significant departure from chemical equilibrium.

3.3. Isotopic Fractionation

Regardless of sediment concentration and open/closed system characteristics, there was an initial marked decrease in $\delta^{13}\text{C}$ -DIC values relative to the bulk carbonate in all experiments (Figs. 2a–c). Thereafter, the open system 0.01 g L⁻¹ and 5 g L⁻¹ experiments all showed broadly similar patterns of change in $\delta^{13}\text{C}$ -DIC (Figs. 2b,c). $\delta^{13}\text{C}$ -DIC values became

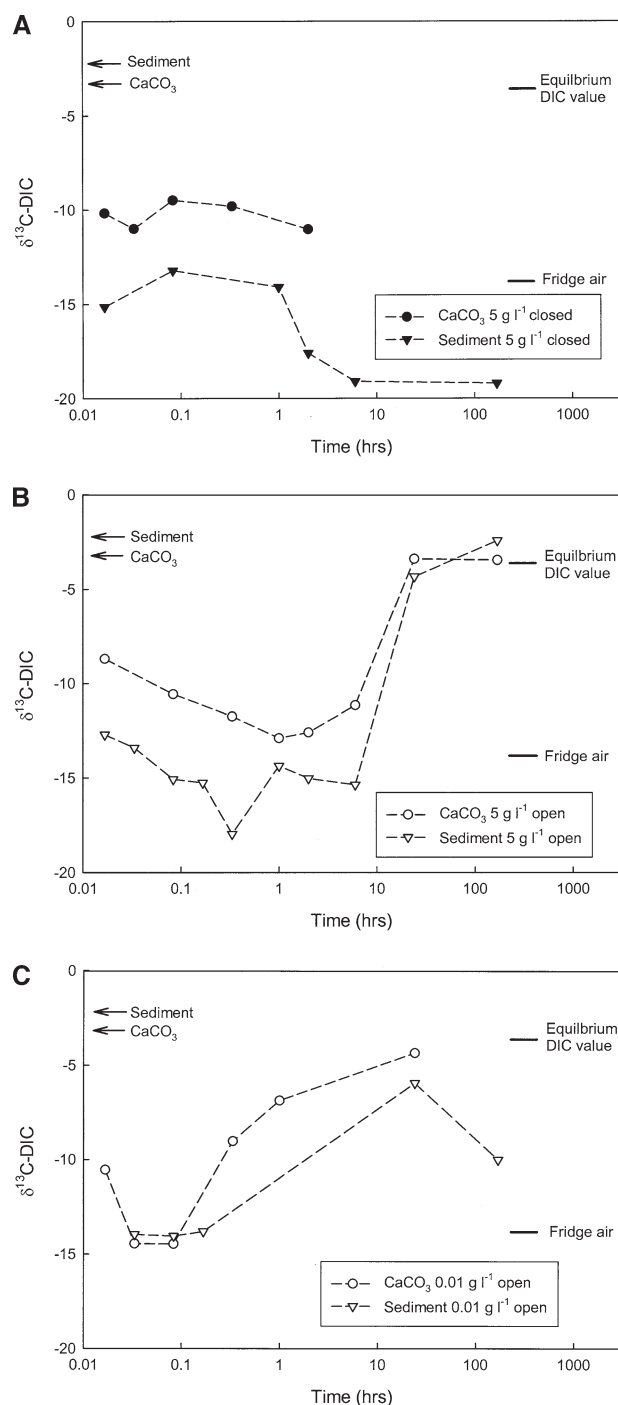


Fig. 2. $\delta^{13}\text{C}$ -DIC vs. time in sediment and CaCO_3 experiments, (a) 5 g L⁻¹ closed system (b) 5 g L⁻¹ open system and (c) 0.01 g L⁻¹ open system. The $\delta^{13}\text{C}$ of the CaCO_3 and carbonate in the glacial sediments (sediment) is noted. The $\delta^{13}\text{C}$ -DIC value in equilibrium with fridge air of -13.8‰ is calculated as -3.6‰ at 5°C, using $\epsilon_{\text{HCO}_3\text{-g}} = 10.2\text{‰}$ (Mook et al., 1974; Zhang et al., 1995).

increasingly negative over the subsequent 0.1–1 h, and then progressively less negative until isotopic equilibrium was reached after ~ 24 h in the CaCO_3 experiments. The secondary negative $\delta^{13}\text{C}$ shift was less prolonged and less pronounced for the 0.01 g L⁻¹ experiments. The $\delta^{13}\text{C}$ shift was greater for the

glacial sediment than for the CaCO_3 where sediment concentrations were the same.

The 24 and 168 h $\delta^{13}\text{C}$ -DIC values were extremely close, -3.4 and -3.5 respectively, in the 5 g L^{-1} CaCO_3 experiment under open system conditions. This was the only experiment in which isotopic equilibrium was clearly attained (Fig. 2b). An experimental equilibrium $\delta^{13}\text{C}$ -DIC value of -3.45‰ (the average of the 24 and 168 h values), yields an equilibrium $\epsilon_{\text{HCO}_3\text{-g}}$ value of 10.35‰ at 5°C , given that the $\delta^{13}\text{C}$ of fridge air was -13.8‰ . This $\epsilon_{\text{HCO}_3\text{-g}}$ value is close to the experimental value determined by Mook et al. (1974) and Zhang et al. (1995) at 5°C (10.2‰). The 5 g L^{-1} sediment experiment was approaching isotopic equilibrium after 24 h (Fig. 2b), but the continued addition of DIC from dissolution of carbonate ($\delta^{13}\text{C} = -2.2\text{‰}$) up until 168 h likely accounts for the final $\delta^{13}\text{C}$ -DIC value, which was heavier than that of experimental equilibrium ($\sim -3.45\text{‰}$) (Figs. 1a,d and 2b).

3.4. $\delta^{13}\text{C}$ Variations in Relation to Weathering Reactions

The closed system experiments provide a measure of the isotopic fractionation associated with carbonate hydrolysis, whereas the open system experiments provide information on additional isotopic fractionation effects due to carbonate dissolution driven by the influx of atmospheric CO_2 .

3.4.1. Carbonate Hydrolysis

The DIC and $P\text{CO}_2$ data demonstrate that carbonate hydrolysis is the main weathering reaction throughout the closed system experiments, and in the first minute of the open system 5 g L^{-1} experiments (Figs. 1a,b). Carbonate is the dominant source of DIC during carbonate hydrolysis (see Eqn. 1). However, the $\delta^{13}\text{C}$ -DIC is significantly lighter than that of the bulk carbonate, suggesting a potential kinetic fractionation process associated with carbonate hydrolysis (Fig. 2a). An initial negative $\delta^{13}\text{C}$ departure due to carbonate hydrolysis is also evident in the open system experiments (Figs. 2b,c). The following analysis predicts the $\delta^{13}\text{C}$ -DIC for the 5 g L^{-1} closed system experiments assuming that there is no isotopic fractionation of the carbonate. The results are compared to the measured values to assess the magnitude of these kinetic fractionation processes.

DIC concentrations were determined for five time steps in each closed system experiment using PHREEQC (Parkhurst and Appelo, 1999) with measured ion concentrations and pH as inputs. Eqn. 4 was used to predict $\delta^{13}\text{C}$ -DIC for the 5 g L^{-1} closed system experiments:

$$\delta_{\text{DIC}}[\text{DIC}] = \delta_{\text{carb}}[\text{DIC}_{\text{carb}}] + \delta_i[\text{DIC}_i] + \delta_{\text{atm}}[\text{DIC}_{\text{atm}}] \quad (4)$$

where items in brackets indicate concentration in moles.

For the CaCO_3 experiments, $[\text{DIC}_{\text{carb}}] = \text{DIC}$ from the powdered carbonate, equal to $[\text{Ca}^{2+}]$ (see Eqn. 1), $\delta_{\text{carb}} = -3.3\text{‰}$, and for the sediment experiments, $[\text{DIC}_{\text{carb}}] = \text{DIC}$ from the carbonate sediment, equal to $[\text{Ca}^{2+}] + [\text{Mg}^{2+}] - [\text{SO}_4^{2-}]$ since dolomite, calcite and gypsum are present in the sediment. And $\delta_{\text{carb}} = -2.15\text{‰}$. The noncarbonate (atmospheric) DIC has been split into two components: (1) $[\text{DIC}_i] = \text{initial DIC}$ of the solution before addition of the sediment. Pure water in equilibrium with atmospheric $P\text{CO}_2$ ($10^{-3.5}$ atm) has a $[\text{DIC}]$ of $27 \mu\text{M}$. This value is assumed to be constant; and (2)

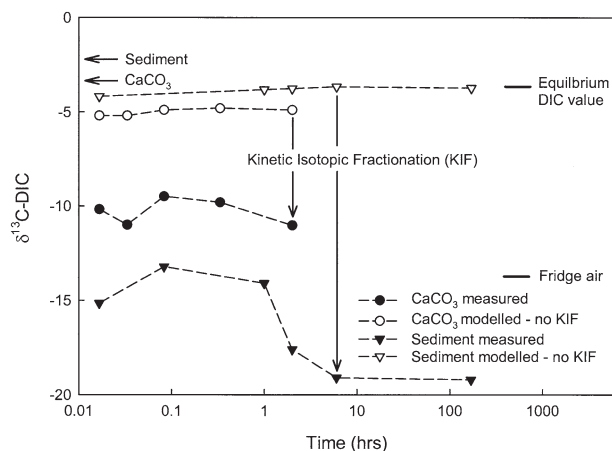


Fig. 3. Predicted $\delta^{13}\text{C}$ -DIC values vs. measured values for the 5 g L^{-1} closed system experiments. The difference between the predicted and measured values is due to kinetic isotopic fractionation, which has a greater effect on $\delta^{13}\text{C}$ -DIC for the glacial sediment compared to the CaCO_3 .

$\delta_i = -3.6\text{‰}$, the $\delta^{13}\text{C}$ -DIC value in equilibrium with the laboratory air. $[\text{DIC}_{\text{atm}}] = \text{DIC}$ from influxing CO_2 in the head space of the bottle. The amount of influxing CO_2 is limited to $\sim 30 \mu\text{M}$, since the head space air was $\sim 3 \text{ cm}^3$ in the closed system bottles and 1 cm^3 air contains $\sim 10 \mu\text{M}$ CO_2 . On average, $27 \mu\text{M}$ CO_2 dissolves into solution indicating that there is almost quantitative mass transfer of CO_2 from the head space to the solution. Therefore, the $\delta^{13}\text{C}$ -DIC from the influxing CO_2 will be that of the head space (laboratory air = -13.8‰) without any fractionation: $\delta_{\text{atm}} = -13.8\text{‰}$.

The predicted average $\delta^{13}\text{C}$ -DIC without any kinetic isotopic fractionation is $-5.0\text{‰} \pm 0.2$ for the closed system 5 g L^{-1} CaCO_3 experiments. The measured isotopic values are on average $\sim -5.3\text{‰}$ lighter, at -10.3‰ (Fig. 3). The predicted average is only $-6.6\text{‰} \pm 0.2$, even if the initial $\delta^{13}\text{C}$ -DIC (δ_i) is assumed to be -13.8‰ , i.e., not in isotopic equilibrium with the laboratory air. This is still 4.2‰ heavier than the measured values. The predicted average $\delta^{13}\text{C}$ -DIC with no kinetic isotopic fractionation is -3.8‰ for the closed system 5 g L^{-1} sediment experiments. This is significantly heavier than the average measured value of -16.1‰ (Fig. 3). These results suggest kinetic fractionation processes are occurring during carbonate hydrolysis. It seems most likely that the kinetic fractionation is associated with the carbonate since it is the dominant DIC source. However, the atmospheric contribution to DIC may also be isotopically light.

The following analysis evaluates the isotopic composition of the initial atmospheric CO_2 component (δ_i) if it, rather than the carbonate is the source of the isotopically light $\delta^{13}\text{C}$ -DIC. δ_i and δ_{carb} are the two potential sources of the isotopically light carbon in the closed system 5 g L^{-1} sediment and CaCO_3 experiments since $[\text{DIC}_{\text{atm}}]$ and δ_{atm} are both constant. Eqn. 4 can be rearranged and solved for δ_i assuming a value for δ_{carb} , or for δ_{carb} , assuming a value for δ_i . The two end member scenarios are as follows. There is no kinetic fractionation of the carbonate in Scenario 1 and $\delta_{\text{carb}} = \text{the bulk carbonate value}$, i.e., δ_i (the initial DIC component) is the sole source of the isotopically light $\delta^{13}\text{C}$ -DIC. Kinetic fractionation of δ_{carb} is the

Table 1. Predicted δ_i and δ_{carb} values for Scenarios 1 and 2 during carbonate hydrolysis (see text for additional details).

Scenario	Experiment	δ_{carb} (‰)	δ_i predicted (‰)
1: No kinetic fractionation is associated with the carbonate	CaCO ₃	-3.3	-37.2
	Sediment	-2.15	-56.5
		δ_{carb} predicted	δ_i
2: The carbonate is the sole source of any kinetic fractionation effect	CaCO ₃	-11.1	-3.6
	Sediment	-19.6	-3.6

sole source of the isotopically light $\delta^{13}\text{C}$ -DIC in Scenario 2, with $\delta_i = -3.6\text{‰}$, the initial DIC component in equilibrium with the fridge atmosphere. The predicted values for δ_i range from -37.2 to -56.5‰ in Scenario 1 and for δ_{carb} they range from -11.1 to -19.6‰ in Scenario 2 (Table 1).

The DIC in the water initially in equilibrium with the laboratory atmosphere is unlikely to be the source of the isotopically light carbon for two reasons. First, it is difficult to envisage a scenario where the laboratory deionized water would contain DIC as isotopically depleted as -56.5‰ (Table 1). Such light isotopic values for DIC have not been reported in the literature. Second, the CaCO₃ and sediment experiments were undertaken within the same week, and thus significant variability in the $\delta^{13}\text{C}$ -DIC (-37.2 to -56.5‰) in the water supply would be required between the two experiments. Physically, it is more plausible that the carbonate is the source of the light carbon and it is also the largest component of the DIC budget, especially in the sediment experiments. The small grain size ($<63\ \mu\text{m}$) of the CaCO₃ and sediment creates a large surface area and thus, a large number of potential reaction sites, which provides an explanation for the kinetic fractionation process. Ca¹²CO₃ weathers preferentially with respect to Ca¹³CO₃, since less energy is required to break the molecular bonds of Ca¹²CO₃. This kinetically selective process is significant in these experiments, due to the abundance of reaction sites and the rapidity of the weathering. A kinetic fractionation factor (hereafter ϵ_{carb}) associated with this process can be determined for each experiment assuming that all the fractionation is associated with the carbonate DIC component (Scenario 2 above). Average δ_{carb} values of -11.1‰ (CaCO₃) and -19.6‰ (sediment) were calculated such that the predicted values equal the measured $\delta^{13}\text{C}$ -DIC values (Table 1). ϵ_{carb} is defined as the difference between the calculated δ_{carb} value and the $\delta^{13}\text{C}$ of the bulk carbonate. Average ϵ_{carb} values are -7.8‰ for the CaCO₃ experiment and -17.4‰ for the sediment experiment.

The kinetic fractionation process is likely to be proportional to reactive surface area. The magnitude of ϵ_{carb} would then be controlled primarily by the physical properties of the sediment, e.g., grain size and fracture properties. A smaller mean grain size increases the number of reaction sites and thus increases the potential for kinetic fractionation. ϵ_{carb} is significantly greater for the sediment than for the CaCO₃, despite the carbonate concentration being slightly higher in the CaCO₃ experiment (there is a noncarbonate component to the sediment).

The grain size distribution of $<63\ \mu\text{m}$ fraction of subglacial stream sediments used in the experiment is unknown. However, the grain size distribution of the subglacial basal sediments, which are the source for the subglacial stream suspended sediments has been determined. 20% of the $<63\ \mu\text{m}$ fraction of John Evans Glacier basal sediments is in the $<3\ \mu\text{m}$ size fraction and 65% of the $<63\ \mu\text{m}$ fraction is in the size fraction $3\text{--}15.6\ \mu\text{m}$ demonstrating a bias towards the finer size fractions. Grain size data are not available for the CaCO₃, but a smaller grain size and greater reactive surface area in the glacial sediments would account for the larger fractionation factor. Abrasion features, such as strained/shattered crystal lattices and fresh mineral surfaces caused by subglacial grinding of the sediments also enhance potential reaction sites (Anderson et al., 1997) and thus the propensity for kinetic fractionation processes with the glacial sediments. It is possible that part of the larger fractionation factor in the glacial sediments may be attributable to differences in bulk carbonate $\delta^{13}\text{C}$ with grain size. If the $\delta^{13}\text{C}$ of the bulk carbonate in the finer fractions (e.g., $<3\ \mu\text{m}$) which will be the most readily dissolvable, is significantly isotopically lighter than that of the bulk carbonate ($<63\ \mu\text{m}$) then the “actual” fractionation factor would be lower than the calculated value of -17.4‰ . Thus, it is noted that the fractionation factor for the sediment is a maximum value and that it may possibly be a little closer to that from the CaCO₃ experiment.

3.4.2. Carbonation of Carbonates

Carbonate hydrolysis is the dominant weathering process in the first minute of the $5\ \text{g L}^{-1}$ open system experiments with sediment and CaCO₃, thus, it is reasonable to assume that the $0.017\ \text{h}$ $\delta^{13}\text{C}$ -DIC values in these experiments also reflect kinetic isotopic fractionation. Carbonate dissolution driven by the influx of atmospheric CO₂ is the dominant weathering process following carbonate hydrolysis, and is accompanied by a decline in $\delta^{13}\text{C}$ -DIC values. These $\delta^{13}\text{C}$ -DIC values remain low until 6 h (Fig. 2b). The subsequent analysis assesses whether this decline may simply reflect input of isotopically light CO₂ from the fridge atmosphere (-14.8‰) by predicting the $\delta^{13}\text{C}$ -DIC for the period $0.017\text{--}6\ \text{h}$ in the $5\ \text{g L}^{-1}$ CaCO₃ experiment. The approach follows section 3.4.1 (Eqn. 4), with the following modifications. A -1‰ kinetic fractionation across the gas-water interface (Zhang et al., 1995) is included as there is free access to the overlying atmosphere in the open system experiments. Hence, the $\delta^{13}\text{C}$ of the atmospheric CO₂ dissolving into solution (δ_{atm}) is -14.8‰ . $\epsilon_{\text{HCO}_3\text{-g}} = 0\text{‰}$, since the system is clearly far from chemical (and isotopic) equilibrium.

The predictive analysis focuses on the simpler CaCO₃ system, since a) there is potentially less variability in carbonate content and grain size relative to the sediment and b) there is no evidence of calcite precipitation, which complicates the interpretation of the isotopic data. Values for DIC were produced with PHREEQC, using values for pH and alkalinity derived from hyperbolic tangent curve fits to the measured data. Two scenarios were investigated. No kinetic fractionation was assumed in Scenario 1 and $\delta_{\text{carb}} = -3.3\text{‰}$. Kinetic fractionation was assumed in Scenario 2 and $\delta_{\text{carb}} = -11.1\text{‰}$, the average value from the closed system experiments (section 3.4.1).

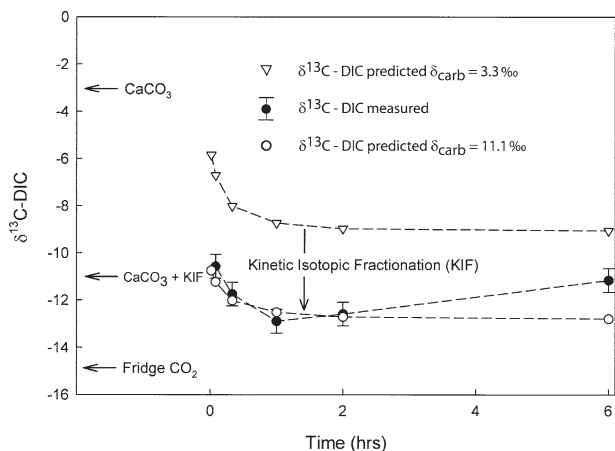


Fig. 4. Predicted and measured $\delta^{13}\text{C-DIC}$ values vs. time for the first 6 h of CaCO_3 5 g L^{-1} weathering experiments. $\delta^{13}\text{C-DIC}$ from CO_2 dissolution = -14.8‰ (fridge $\text{CO}_2 = -13.8\text{‰}$, + $\epsilon_k = -1\text{‰}$). Error bars are $\pm 0.5\text{‰}$.

The predicted $\delta^{13}\text{C-DIC}$ values which incorporate kinetic fractionation provide a good fit to the experimental data for the first 6 h whereas the values without kinetic fractionation are $\sim 4\text{‰}$ heavier than the measured values (Fig. 4). These results suggest two important conclusions regarding carbon isotope behavior during the initial 6 h of carbonate dissolution driven by the influx of atmospheric CO_2 . First, the magnitude of kinetic isotopic fractionation is similar to that observed during carbonate hydrolysis. Second, there is no equilibrium fractionation of the influx of atmospheric CO_2 . A minor caveat is that the 6 h value is slightly heavier (1.6‰) than predicted. This may reflect one, or a combination of, the following two processes. First, the impact of kinetic isotopic fractionation on δ_{carb} will decline through time as continued dissolution of the sediment produces increasingly heavy $\delta^{13}\text{C}$ values, since there must be conservation of isotope mass balance. Second, as rates of CO_2 ingress decrease a degree of equilibrium isotopic fractionation may be occurring such that $\epsilon_{\text{HCO}_3\text{-g}} > 0\text{‰}$. Rates of C input from both the atmosphere and rock are significantly reduced in the period 2–6 h, compared to the initial phase of the experiment (Fig. 1a), suggesting that kinetic processes and their isotopic effects are likely to be declining in importance.

3.5. Effect of Carbonate Concentration on Kinetic Isotopic Fractionation

The carbonate concentration of the sediment is a key variable in determining $\delta^{13}\text{C-DIC}$ variations. At low sediment (and carbonate) concentrations ($\leq 0.01 \text{ g L}^{-1}$), the magnitude of ϵ_{carb} is initially the same as at higher carbonate concentrations (Figs. 2b,c). However, kinetic isotopic fractionation is controlled by reactive surface area and thus it can only persist for a short time at low sediment concentrations, since “whole rock” dissolution will dominate more quickly than at higher concentrations and produce $\delta^{13}\text{C-DIC}$ values similar to the bulk rock value. This is evident in the 0.01 g L^{-1} experiments Figure 2c, where the return to isotopic equilibrium following carbonate hydrolysis occurs earlier than in the equivalent 5 g L^{-1} experiment (Fig. 2b).

4. CONCLUSIONS

1. The weathering experiments demonstrate a previously unknown kinetic isotopic fractionation process that occurs during the initial stages of carbonate weathering. Kinetic isotopic fractionation occurs during carbonate hydrolysis and persists for at least the first 6 h of carbonate dissolution driven by the influx of atmospheric CO_2 . Kinetic isotopic fractionation is determined by reactive surface area, and the magnitude of ϵ_{carb} associated with this process is controlled primarily by the physical properties of the sediment (e.g., grain size and fracture properties). ϵ_{carb} may be as high as -17.4‰ for the initial stages of weathering of carbonate-rich glacial sediments. Therefore, in natural environments where rock:water contact times are short $< 6\text{--}24 \text{ h}$ (e.g., glacial systems, headwaters in fluvial catchments) and there is excess carbonate in the sediments, kinetic fractionation processes will likely dominate the $\delta^{13}\text{C-DIC}$ signal. Hence, in these types of environment it will be difficult to apply conventional isotope mass balance techniques to identify microbial CO_2 signatures in DIC from $\delta^{13}\text{C-DIC}$ data.

2. PCO_2 equilibrium occurs significantly faster than isotopic equilibrium in all the open system weathering experiments, regardless of carbonate concentration. Thus, PCO_2 values may be only a coarse guide to isotopic equilibrium conditions. Equilibrium isotopic fractionation between the influx of CO_2 and HCO_3^- does not occur for at least the first 6 h of the carbonation reaction, such that $\epsilon_{\text{HCO}_3\text{-g}} \sim 0$ during this time. This is considerably longer than previously reported, e.g., Szaran (1997), albeit under slightly different initial experimental conditions.

Acknowledgments—This work was funded by an NSERC (Canada) operating grant to Sharp and by a Geological Society of America grant to Skidmore. We thank S. Bottrell for constructive comments on an earlier draft of the manuscript and K. Muehlenbachs for helpful discussions and advice on laboratory techniques. We appreciate the constructive reviews from three anonymous referees and the associate editor.

Associate editor: K. Kyser

REFERENCES

- Amiotte-Suchet P., Aubert D., Probst J. L., Gauthier-Lafaye F., Probst A., Andreux F., and Viville D. (1999) $\delta^{13}\text{C}$ pattern of dissolved inorganic carbon in a small granitic catchment: The Strengbach case study (Vosges Mountains, France). *Chem. Geol.* **159**, 129–145.
- Anderson S. P., Drever J. I., and Humphrey N. F. (1997) Chemical weathering in glacial environments. *Geology* **25**, 399–402.
- Anderson S. P., Drever J. I., Frost C. D., and Holden P. (2000) Chemical weathering in the foreland of a retreating glacier. *Geochim. Cosmochim. Acta* **64**, 1173–1189.
- Blum J. D. and Erel Y. (1995) A silicate weathering mechanism linking increases in marine $^{87}\text{Sr}/^{86}\text{Sr}$ with global glaciation. *Nature* **373**, 415–418.
- Bottrell S. H. and Tranter M. (2002) Sulphide oxidation under partially anoxic conditions at the bed of the Haut Glacier d’Arolla, Switzerland. *Hydrol. Proc.* **16**, 2363–2368.
- Brantley S. L., Chesley J. T., and Stillings L. L. (1998) Isotopic ratios and release rates of strontium measured from weathering feldspars. *Geochim. Cosmochim. Acta* **62**, 1493–1500.
- Brown G. H., Sharp M., Tranter M., Gurnell A. M., and Nienow P. W. (1994) Impact of post-mixing reactions on the major ion chemistry of bulk meltwaters draining the Haut Glacier d’Arolla, Valais, Switzerland. *Hydrol. Proc.* **8**, 465–480.

- Chou L., Garrels R. M., and Wollast R. (1989) Comparative study of the kinetics and mechanisms of dissolution of carbonate minerals. *Chem. Geol.* **78**, 269–282.
- Craig H. (1957) Isotopic standards for carbon and oxygen and correction factors for mass spectrometric analysis of carbon dioxide. *Geochim. Cosmochim. Acta* **12**, 133–149.
- Deines P. D., Langmuir D., and Harmon R. S. (1974) Stable carbon isotope ratios and the existence of a gas phase in the evolution of carbonate groundwaters. *Geochim. Cosmochim. Acta* **38**, 1147–1164.
- Dreybrodt W., Lauckner J., Zaihua L., Svensson U., and Buhmann D. (1996) The kinetics of the reaction $\text{CO}_2 + \text{H}_2\text{O} \rightarrow \text{H}^+ + \text{HCO}_3^-$ as one of the rate-limiting steps for the dissolution of calcite in the system $\text{H}_2\text{O}-\text{CO}_2-\text{CaCO}_3$. *Geochim. Cosmochim. Acta* **60** (18), 3375–3381.
- Deuser W. G. and Degens E. T. (1967) Carbon isotope fractionation in the system CO_2 (gas)- CO_2 (aqueous)- HCO_3^- (aqueous). *Nature* **215**, 1033–1035.
- Fairchild I. J., Bradby L., Sharp M., and Tison J.-L. (1994) Hydrochemistry of carbonate terrains in alpine glacial settings. *Earth Surf. Proc. Landforms* **19**, 33–54.
- Fairchild I. J. and Killawee J. A. (1995) Selective leaching in glacierized terrains and implications for retention of primary chemical signals in carbonate rocks. In *Proceedings of the 8th International Symposium on Water-Rock Interaction* (eds. Y. K. Kharaka and O. V. Chudaev), pp. 79–82. Balkema.
- Fairchild I. J., Killawee J. A., Hubbard B., and Dreybrodt W. (1999) Interactions of calcareous suspended sediment with glacial meltwater: A field test of dissolution behaviour. *Chem. Geol.* **155**, 243–263.
- Faure G. (1986) Principles of Isotope Geology. Wiley.
- Gibbs M. T. and Kump L. R. (1994) Global chemical erosion during the last glacial maximum and the present: Sensitivity to changes in lithology and hydrology. *Paleoceanography* **9**, 529–543.
- Hodson A. J., Tranter M., and Vatne G. (2000) Contemporary rates of chemical denudation and atmospheric CO_2 sequestration in glacier basins: An Arctic perspective. *Earth Surf. Proc. Landforms* **25**, 1447–1471.
- McCrea J. M. (1950) On the isotope chemistry of carbonates and a paleotemperature scale. *J. Chem. Phys.* **18**, 849–857.
- Mills G. A. and Urey H. C. (1940) The kinetics of isotope exchange between carbon dioxide, bicarbonate ion, carbonate ion and water. *J. Am. Chem. Soc.* **62**, 1019–1026.
- Mook W. G., Bommerson J. C., and Staverman W. H. (1974) Carbon isotope fractionation between dissolved bicarbonate and gaseous carbon dioxide. *Earth Planet. Sci. Lett.* **22**, 169–176.
- Parkhurst D. L. and Appelo C. A. J. (1999) *User's Guide to PHREEQC (Version 2)—A Computer Program For Speciation, Batch-Reaction, One-Dimensional Transport, and Inverse Geochemical Calculations*. U.S. Geological Survey.
- Raiswell R. (1984) Chemical Models of solute acquisition in glacial melt waters. *J. Glaciol.* **30**, 49–57.
- Sharp M. (1996) Weathering pathways in glacial environments: Hydrological and lithological controls. (ed. S. Bottrell) *Proceedings of the fourth International Symposium on the Geochemistry of the Earth's Surface*. Leeds University Press, Leeds, UK pp. 652–655.
- Sharp M. J., Tranter M., Brown G. H., and Skidmore M. (1995) Rates of chemical denudation and CO_2 drawdown in a glacier-covered alpine catchment. *Geology* **23**, 61–64.
- Sharp M., Parkes J., Cragg B., Fairchild I. J., Lamb H., and Tranter M. (1999) Widespread bacterial populations at glacier beds and their relationship to rock weathering and carbon cycling. *Geology* **27**, 107–110.
- Skidmore M. L. (1995) The hydrochemistry of a high Arctic glacier. MSc. thesis. University of Alberta.
- Skidmore M. L. and Sharp M. J. (1999) Drainage behaviour of a high Arctic polythermal glacier. *Ann. Glaciol.* **28**, 209–215.
- Skidmore M., Foght J., and Sharp M. (2000) Microbial life beneath a high Arctic glacier. *Appl. Environ. Microbiol.* **66**, 3214–3220.
- Stumm W. and Morgan J. J. (1996) *Aquatic Chemistry: Chemical Equilibria and Rates in Natural Waters*. Wiley-Interscience.
- Szaran J. (1997) Achievement of carbon isotope equilibrium in the system HCO_3^- (solution)- CO_2 (gas). *Chem. Geol.* **142**, 79–86.
- Telmer K. and Veizer J. (1999) Carbon fluxes, pCO_2 and substrate weathering in a large northern river basin, Canada: Carbon isotope perspectives. *Chem. Geol.* **159**, 61–86.
- Tranter M., Sharp M. J., Lamb H. R., Brown G. H., Hubbard B. P., and Willis I. C. (2002) Chemical weathering at the bed of Haut Glacier d'Arolla, Switzerland—A new model. *Hydrol. Proc.* **16**, 959–993.
- Vogel J. C., Grootes P. M., and Mook W. G. (1970) Isotopic fractionation between gaseous and dissolved carbon dioxide. *Zeitschr. Phys.* **230**, 225–238.
- Wendt I. (1968) Fractionation of carbon isotopes and its temperature dependence in the system CO_2 -Gas- CO_2 in solution and HCO_3^- - CO_2 in solution. *Earth Planet. Sci. Lett.* **4**, 64–68.
- White A. F., Bullen T. D., Vivit D. V., Schulz M. S., and Clow D. W. (1999) The role of disseminated calcite in the chemical weathering of granitoid rocks. *Geochim. Cosmochim. Acta* **63**, 1939–1953.
- Zhang J., Quay P. D., and Wilbur D. O. (1995) Carbon isotope fractionation during gas-water exchange and dissolution of CO_2 . *Geochim. Cosmochim. Acta* **59**, 107–114.